Eclogite facies relics in metabasites from the Sierra de Guadarrama (Spanish Central System): *P-T* estimations and implications for the Hercynian evolution

L. BARBERO[1,*] AND C. VILLASECA[2]

[1] Departamento de Geología, Facultad C. C. del Mar, Universidad de Cádiz, 11510 Puerto Real, Cádiz, Spain
[2] Departamento de Petrología y Geoquímica, Facultad C. C. Geológicas, Universidad Complutense, 28040 Madrid, Spain

Relics of *HP-MT* eclogitic assemblages related to the first metamorphic stage of the Hercynian orogeny in the Sierra de Guadarrama (Spanish Central System, SCS) are preserved as boudins of pre-Ordovician metabasites enclosed by felsic gneisses. Textures indicate a multi-stage metamorphic history starting in the *MT* eclogite facies (as deduced from the presence of omphacite and rutile included in garnet) and continuing through medium to low pressure granulite and retrograde amphibolite-greenschist facies. Thermobarometric calculations in the eclogitic paragenesis yield pressures of ~14 kbar for temperatures in the range 725–775°C. Thermobarometry for the subsequent granulitic stage indicates a significant drop in pressure ($P < 10$ kbar) for similar temperatures of ~750°C. Metabasites vary from gabbro to leucotonalites showing the typical Fe enrichment of the tholeiitic series. Chemical characteristics indicate a derivation from low-pressure crystallization of tholeiitic melts more enriched than typical MORB compositions. Their original location far from continental margins as evidenced by the absence of ophiolitic material in the area and their association with platform sediments suggests that eclogitization was related to intracontinental crustal subduction and thickening. The *P-T* conditions estimated in the metabasites for the first metamorphic stage are similar to ones deduced for the surrounding metasediments and suggest that the Hercynian crust could have reached a thickness of ~70–80 km, which is more than the double the present thickness.

KEYWORDS: eclogite assemblage, Spanish Central System, Hercynian evolution, MORB.

Introduction

THE Sierra de Guadarrama is located in the axial zone of the Iberian branch of the Hercynian belt (Fig. 1) in the so-called Central Iberian Zone (San José *et al.*, 1990). This sector represents a typical intracontinental setting as seen from its location far from recognized ophiolitic complexes or supposed continental margins. The nearest ophiolitic complex of the Badajoz-Córdoba shear zone is located >320 km to the southwest even after the shortening which occurred during the Hercynian orogeny. The metamorphic evolution related to the Hercynian orogeny is characterized by three stages of re-crystallization related to a single metamorphic cycle (Villaseca, 1983; Arenas *et al.*, 1991). The initial metamorphism (M_1) coincides with the first and with part of the second deformative events (D_1 and D_2) and is characterized by a medium *P-T* regime associated with crustal thickening and progressive burial. The most characteristic large-scale D_1 compressional structure in the study area is a series of km-scale ductile shear zones of orthogneisses imbricated with thin sheets of metasediments (Fig. 1) (Macaya *et al.*, 1991). In previous works, the precise metamorphic conditions of M_1 have not been established precisely, which was explained as a consequence of the overprinting by the second metamorphic stage (M_2). Villaseca

* E-mail: luis.barbero@uca.es

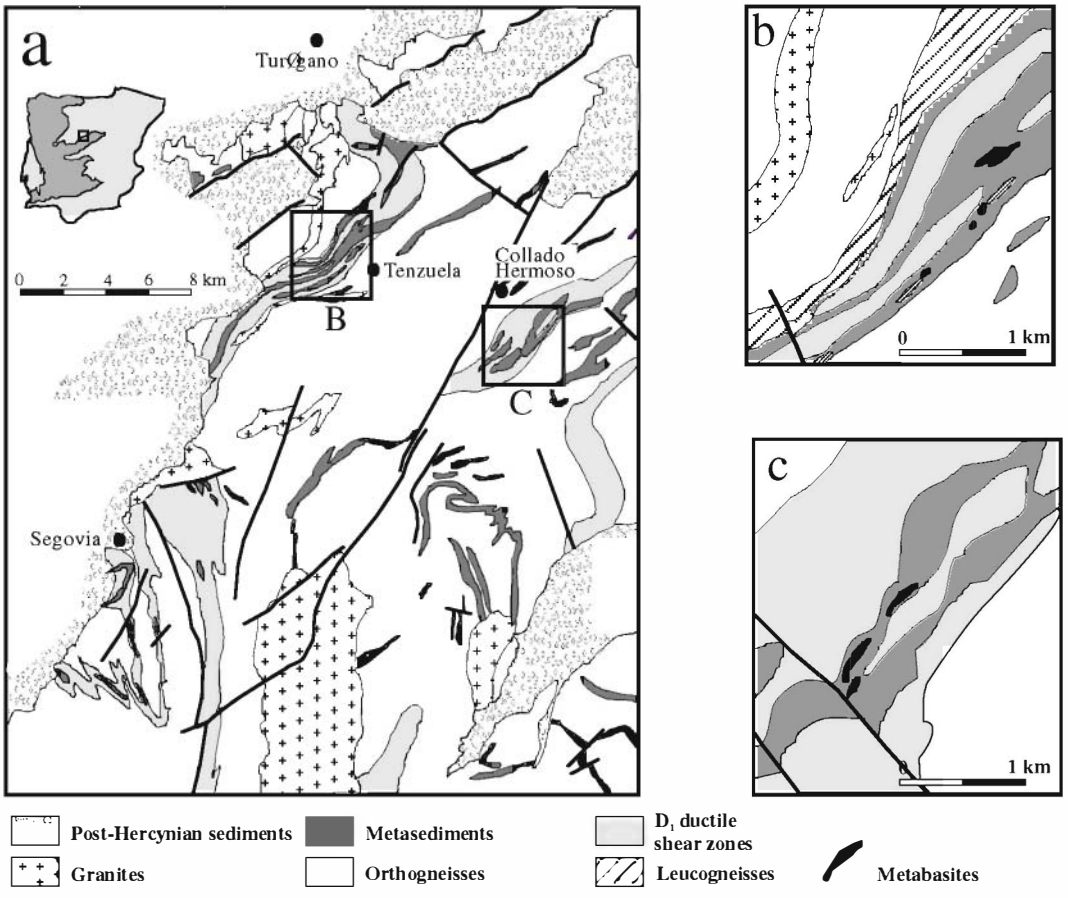

FIG. 1. (*a*) Geological map of a sector of the Central Spain Region (Hercynian orogen) and its location in the Iberian Hercynian Belt (grey area). The two insets are the main regions where the studied metabasites crop out; (*b*) the Tenzuela sector; and (*c*) the Collado Hermoso sector.

(1983) describes these metabasic rocks as having a relict eclogitic assemblage, citing the presence of Na-rich pyroxenes included in garnets. The maximum pressure attained was estimated to be ~7–11 kbar. In a more recent work on these metabasites, Villaseca and Barbero (1994) made a brief revision of the *PT* conditions of the first Hercynian metamorphic episode concluding that the minimum pressure achieved was ~9 kbar, probably reaching up to 12–15 kbar for temperatures in the range 650–750°C. The second metamorphic stage (M_2, paroxysmal metamorphism) coincides with the final development of the second deformation episode (D_2), which is essentially an extensional event which overprints and transposes D_1 structures generating some km-scale ductile extensional shear zones such as the Berzosa-Riaza zone to the east of the studied area (Escuder Viruete *et al.*, 1998). During M_2, this orogenic segment reached the highest temperature (715°C, 4–5 kbar, Villaseca, 1983; Arenas *et al.*, 1991) and a decompressional evolution occurred. Mineral parageneses of the M_2 stage are generally well preserved and define a granulite facies metamorphic zone with orthoclase, cordierite and sillimanite. Migmatization occurred mainly in the quartzo-feldspathic meta-igneous and metapelitic protoliths associated with these metabasites. In nearby granulitic terranes such as the Anatectic Complex of Toledo located 100 km to the south of the study area, the metamorphic climax reached 800 ± 50°C and

5 ± 1 kbar (Barbero, 1995). Finally, a third metamorphic stage (M_3), produced a retrogression of the previous parageneses during the last decompressional stage. The M_3 mineral assemblages reflect greenschist facies conditions of ~450°C and 2 kbar (Villaseca, 1983; Arenas *et al.*, 1991).

In the present work, new mineral chemical data on the relict eclogitic paragenesis of the M_1 metamorphic stage are presented with the aim of determining the *P-T* eclogitic conditions attained during the Hercynian metamorphic evolution of this area. Moreover, new whole-rock chemical data on these metabasites have been obtained which, together with previous data (Villaseca, 1983; Villaseca *et al.*, 1993), may place constraints on the significance of the basic magmatism during pre-Ordovician times.

Geological setting

The Sierra de Guadarrama is composed mainly of metamorphic rocks, both metasedimentary and meta-igneous types, into which voluminous peraluminous late Hercynian granites intruded (Fig. 1).

The metasedimentary sequences, of uncertain age, crop out under the Sardic unconformity (Lower Ordovician–Middle Devonian). Significant palaeontological remains are absent, which together with the fact that these sedimentary sequences are intruded by many pre-Ordovician meta-igneous rocks, make stratigraphic correlation very difficult. A succession of schists and paragneisses, with quartzites, and discontinuous layers of marbles, amphibolites and calc-silicate rocks form the majority of the series. This series of Proterozoic age is assigned to the so-called Complejo Esquisto Grauváquico of the Central Iberian Zone (San José *et al.*, 1990). The presence of abundant layers of metapelites with a hornfels-like appearance surrounded by meta-igneous types is characteristic. These meta-igneous types comprise different augen, porphyritic, and leucocratic varieties intruded into the pre-Ordovician sedimentary sequence, described previously. Geochronological data obtained from orthogneissic rocks suggest an early Ordovician age (470–500 Ma Rb-Sr whole rock, Vialette *et al.*, 1987; ~487 Ma, U-Pb zircon Valverde-Vaquero *et al.*, 1995). These Lower Ordovician orthogneisses are mainly acidic varying from granodioritic to leucogranitic types. Almost all of them have a peraluminous composition with a tendency to be more peraluminous towards more basic compositions, thus having S-type characteristics.

Two types of basic meta-igneous rocks appear in the area, both of them restricted exclusively to the central domain of the Sierra de Guadarrama. The metabasites with eclogitic relics have never been found interlayered within the abundant lower Ordovician orthogneisses (Fig. 1). These older metabasites crop out as discontinuous bands, boudins or lenses within the Precambrian metasediments against which they present sharp contacts. They were intensively recrystallized during the Hercynian orogeny, being transformed into amphibolitic gneisses and garnetiferous mela-amphibolites. Based on several characteristics (discussed below) they are interpreted as being derived from tholeiitic sills of undetermined Precambrian age, at least previous to the orthogneisses of Lower Ordovician age. A significant variation in composition from gabbros towards leucotonalites is observed (Villaseca, 1983). It is only in these metabasites in which the residual eclogitic mineral assemblages studied in the present work appear.

A second group of metabasites, composed of coronitic metagabbros and metadiorites, intruded into all of the previous stratigraphic series (not alone into the metasedimentary Proterozoic sequences, but also into the Lower Ordovician felsic orthogneisses). Because of their tendency to appear in shear zones related to the compressional deformation stage, they have been interpreted to be early Hercynian in age, associated with the Hercynian crustal thickening (Villaseca, 1985). These coronitic metagabbros, in contrast to the metabasites described previously, are not as intensely re-crystallized, and some of them even preserve clear igneous textures in the internal zones of the massifs. No evidence of important high-pressure re-crystallization has been found in this metabasite and garnet-bearing varieties are very rare. They are interpreted as syn-orogenic continental tholeiitic sills because of their low alkalies and high Ti and Fe contents (Villaseca, 1985).

Analytical methods

For this study, ~50 samples of amphibolitic metabasites from the region of Turégano (near Segovia, Fig. 1) were investigated petrographically. The mineral assemblages are summarized in Table 1. Electron microprobe analyses were performed on seven polished sections using three different microprobes: a JEOL

TABLE 1. Relation of the blastesis of the different mineral phases with respect to the three metamorphic stages of the Spanish Central System.

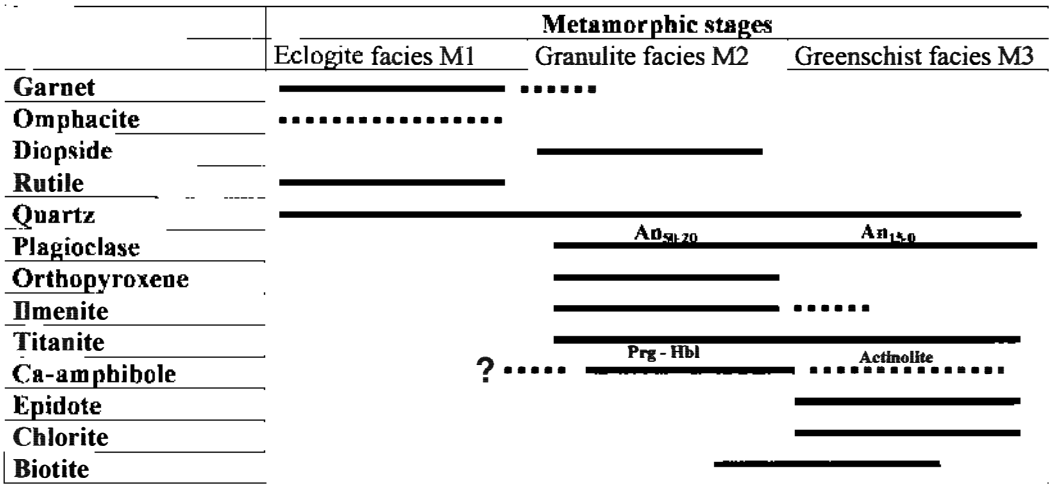

SUPERPROBE JXA 8900-M at Complutense University of Madrid; a JEOL SUPERPROBE 733 at St. Andrews University (UK); and a CAMECA SX-50 at Oviedo University (Spain). In all cases, the operating conditions were 15 kV, 20 nA, and a beam diameter of 2–5 μm, and ZAF correction procedure was used. Analyses performed on the same mineral grain in the different microprobes gave similar results.

Whole-rock major elements were determined by ICP-AES and trace elements by ICP-MS at CNRS (Nancy, France) following the method of Govindaraju and Mevelle (1987). Three whole-rock chemical analyses have been taken from Villaseca (1983) (Table 5). The mineral abbreviations follow those used by Kretz (1983).

Sample description

Metabasic rocks containing high-pressure relics appear in the Turégano region (Fig. 1) as boudins of variable size included in the metasediments. The largest outcrop occurs near Tenzuela (Fig. 1*b*) where a varied and complex massif of metabasites of ~2000 m^2, showing concordant sharp contacts with the surrounding metapelites and marbles, is exposed. In this massif, several types can be distinguished: granoblastic leuco-amphibolites with varied grain size; foliated mela-amphibolites interlayered with the former leucocratic types; and medium- to fine-grained garnet-bearing amphibolites with a massive structure and an eclogite-like appearance, generally found as rounded masses included within the former rock types. Some pegmatitic varieties with conspicuous amphibole, plagioclase and quartz crystals appear. A second important group of small outcrops of metabasites are located to the south of the Collado Hermoso village (Fig. 1*c*).

Different mineral assemblages, which are the result of the successive metamorphic recrystallization stages, can be distinguished. In Table 1 the relation between the blastesis of the different mineral phases and the three metamorphic stages of the area are summarized.

Eclogitic relict paragenesis

This comprises minerals grown during the M_1 stage including garnet, Na-rich-clinopyroxene, amphibole (?), ilmenite (?), rutile and apatite. Most of these minerals are found as inclusions in garnet domains.

Granulitic paragenesis

This was imposed on the previous assemblage; plagioclase, clinopyroxene (low-Na), orthopyroxene, amphibole and some biotite and K-feldspar in the more felsic varieties appear. These phases are related to the second metamorphic re-crystallization.

Finally, the retrogression of the previous assemblages during the M_3 stage produces minerals such as chlorite, actinolite, quartz and epidote (Table 1).

Garnet appears in proportions varying from accessory amounts up to 20% in certain samples (Fig. 2). It is more or less equidimensional and varies in form from euhedral to anhedral (atoll or ameboid forms); grain sizes are up to 2 mm and of sieved textural appearance, as a consequence of the abundant clinopyroxene, quartz, plagioclase, amphibole, orthopyroxene, biotite, apatite, rutile and ilmenite inclusions, usually observed (Fig. 2). In these complex garnet domains, some of these minerals (clinopyroxene, quartz, rutile) should be interpreted as primary inclusions entrapped during the garnet growth. Other inclusions (plagioclase, amphibole, biotite, orthopyroxene, ilmenite) clearly post-date garnet growth and can be interpreted as secondary inclusions or reaction products inside garnet. The presence of plagioclase coronas around clinopyroxene inclusions (Fig. 2*d*) suggests that the plagioclase enclosed in garnet could have re-crystallized during the second metamorphic stage, as could also be the case for the orthopyroxene, amphibole, biotite, ilmenite and quartz. The presence of a continuous plagioclase corona around garnet, sometimes with symplectitic intergrowths with amphibole and/or ilmenite in the external part of the corona (Fig. 2*c*), is clearly related to the M_2 recrystallization. In the most retrograde eclogites, where garnet and clinopyroxene have been almost completely destroyed, granoblastic plagioclase aggregates develop an exsolution-like texture as seen in the alignment of tiny needle-like inclusions of apatite and diopsidic clinopyroxene.

It is possible to find omphacitic clinopyroxene as relics of the M_1 paragenesis (as discussed in the mineral chemistry section), thus reflecting high-pressure conditions. Clinopyroxene is found either as small inclusions in the garnet or as euhedral crystals in the matrix, in this case defining, together with the amphibole, plagioclase, orthopyroxene and quartz, the granonematoblastic texture of the rock. A thin plagioclase film usually surrounds clinopyroxene inclusions, which isolates them from the garnet (Fig. 2*d*). Orthopyroxene is much less abundant and appears either as small crystals apparently included in the garnet or more commonly in the matrix. Orthopyroxene is restricted to certain samples from the Tenzuela massif (Fig. 1).

Amphibole is the most abundant ferromagnesian phase in these metabasites. It appears as subhedral granoblastic crystals but also as a continuous rim around ilmenite. It clearly grew later than the garnet, clinopyroxene and some of the plagioclase. Sometimes amphibole appears to be symplectitically intergrown with plagioclase as an incomplete corona around garnet. It also appears as secondary inclusions within garnet, in this case probably representing retrograded transformation of previous clinopyroxene inclusions. In the amphibole-rich varieties it appears as large nematoblastic crystals poikilitically enclosing residual garnet and usually developing a thin plagioclase film between both minerals.

Ilmenite is abundant in several types as elongated crystals in the nematoblastic matrix of the rock. Rutile is only found as inclusions in garnet. Titanite can frequently be found associated with ilmenite. Quartz is another accessory phase in these eclogitic metagabbros. Occasionally clinopyroxene plus plagioclase surround some corroded quartz aggregates.

Mineral chemistry

Garnet

The garnet composition in the metabasites is in the range of almandine (58–69 mol.%), grossular (24–30 mol.%) and pyrope (5–14 mol.%) with subordinate spessartine (<5.5 mol.%) and uvarovite (<0.7 mol.%) (Table 2). Only in one sample from the Collado Hermoso sector (sample 82245), is garnet slightly richer in grossular (30.0 to 33.6 mol.%) and pyrope (12.0 to 14.0 mol.%) components (Fig. 3*a*) reflecting their relatively higher bulk-rock Ca composition. Garnets plot in the field of group C eclogites as defined by Coleman *et al.* (1965) (Fig. 3*a*). The majority of the metabasites contain unzoned garnets (Fig. 3*b*) or garnets in which zoning is not well defined. Nevertheless, when present, zoning is characterized by an increase in Fe and a decrease in Ca from core to rim (samples 82244 and 96897, Fig. 3*c*,*d*). Such zoning may have been caused by a pressure decrease (Raheim and Green, 1975) and is in agreement with the presence of retrograde plagioclase coronas around garnet.

Clinopyroxene

The Fe^{3+} contents in clinopyroxene are estimated, based on charge balance considerations, as the sum of cations is very close to 4 in all cases. As

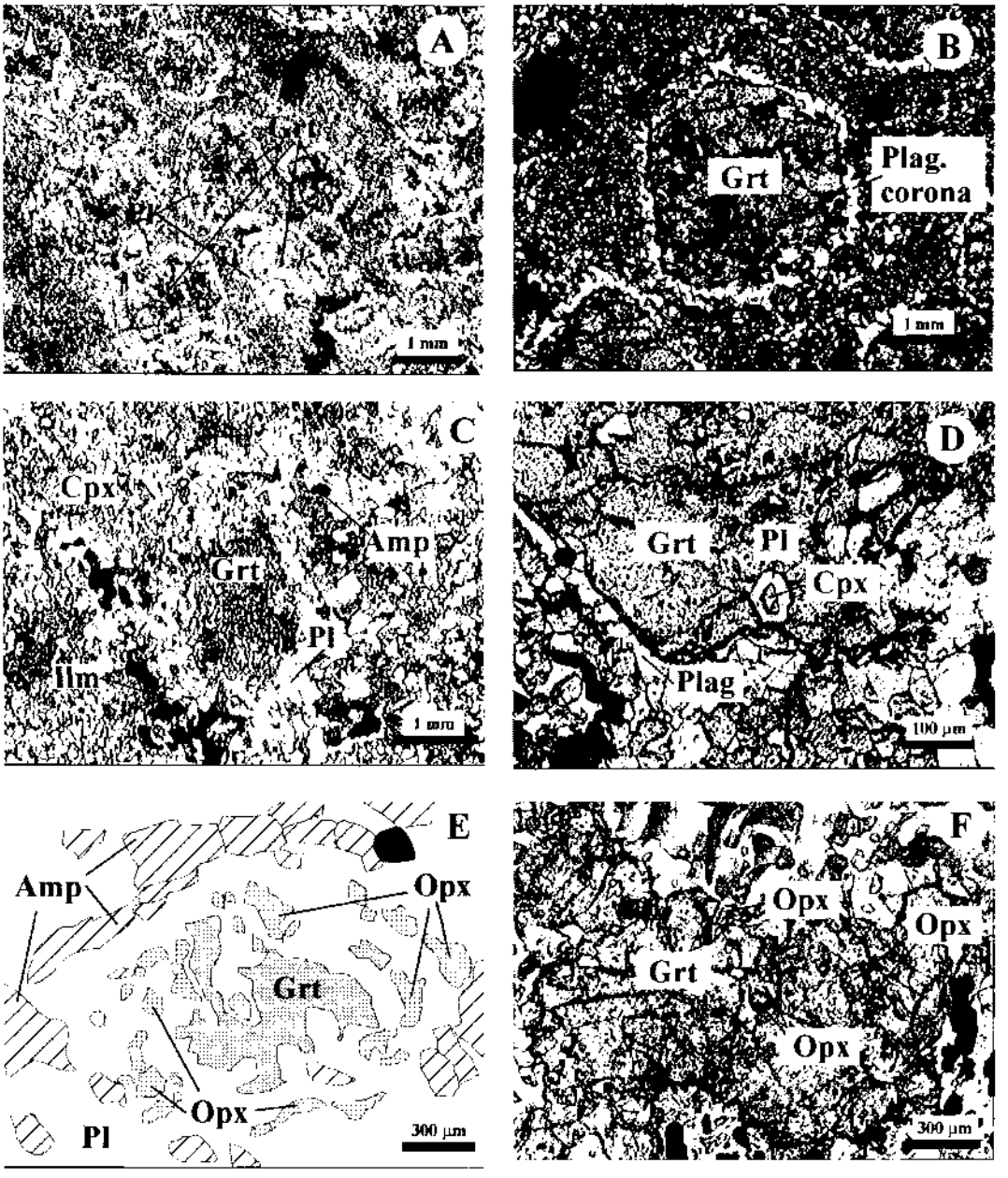

FIG. 2. Microtextural aspects of different metabasites from the studied area. (*a*) General aspect of a retro-eclogite with plagioclase coronas around garnet and abundant ilmenite crystals; the matrix is composed mainly of granoblastic amphibole and plagioclase (sample 82244). (*b*) Detail of a plagioclase corona around a euhedral garnet (sample 71303). (*c*) Metabasite in a more retrograde stage showing a sieved-textured garnet and a coarse-grained granoblastic matrix composed of plagioclase, clinopyroxene, amphibole (also surrounding ilmenite) and ilmenite (sample 96894). (*d*) Detail of an omphacitic clinopyroxene included in garnet with a typical plagioclase corona between both minerals (sample 71300). (*e*) Petrographic scheme drawn from a microphotograph of sample 96894 showing the textural relations of the orthopyroxene (Opx), plagioclase (Pl), and amphibole (Amp) around a corroded garnet crystal. (*f*) Orthopyroxene inclusions in garnet from sample 96895.

TABLE 2. Selected analyses of garnet of tholeiitic metabasites from the Sierra de Guadarrama.

Sample	71300	71300	71300	71300	96895	96895	82244	82244	82244	82244
Analysis	103 rim	104	108	109	71 core	74 rim	69 rim	70	72	73 core
SiO_2	39.02	38.09	38.41	38.81	38.42	38.15	37.02	37.28	37.39	37.68
TiO_2	0.16	0.06	0.15	0.22	0.24	0.20	0.16	0.07	0.29	0.17
Al_2O_3	20.94	20.89	20.82	21.07	20.88	20.84	20.69	21.05	20.89	21.15
FeO	29.88	30.45	29.18	28.39	28.21	29.58	28.27	28.49	28.74	28.14
MnO	1.41	0.94	1.24	1.38	2.45	0.84	0.33	0.45	0.43	0.79
MgO	1.76	1.85	2.41	2.43	1.53	1.86	2.87	2.72	2.71	2.62
CaO	9.64	8.56	9.17	9.43	9.94	9.52	9.77	9.47	9.47	9.76
Na_2O	0.00	0.00	0.10	0.00	0.00	0.00	0.00	0.00	0.00	0.00
Total	102.82	100.83	101.40	101.74	101.66	100.98	99.14	99.53	99.93	100.31
Structural formula O = 12										
Si	3.00	3.00	3.00	3.00	3.00	3.00	2.97	2.98	2.98	2.99
Al^{IV}	0.00	0.00	0.00	0.00	0.00	0.00	0.03	0.02	0.02	0.01
Al^{VI}	1.92	1.95	1.93	1.94	1.94	1.95	1.93	1.96	1.95	1.97
Ti^{VI}	0.01	0.00	0.01	0.01	0.01	0.01	0.01	0.00	0.02	0.01
Mg	0.20	0.22	0.28	0.28	0.18	0.22	0.34	0.32	0.32	0.31
Fe^{2+}	1.94	2.02	1.92	1.86	1.86	1.96	1.90	1.90	1.92	1.87
Mn	0.09	0.06	0.08	0.09	0.16	0.06	0.02	0.03	0.03	0.05
Ca	0.80	0.73	0.77	0.79	0.84	0.81	0.84	0.81	0.81	0.83
End-members										
Prp	6.69	7.23	9.25	9.36	5.92	7.20	11.06	10.55	10.47	10.12
Alm	63.85	66.68	62.76	61.45	61.12	64.40	61.14	62.03	62.29	61.02
Sps	3.06	2.07	2.71	3.03	5.37	1.84	0.72	0.99	0.94	1.74
Grs	26.40	24.01	25.27	26.15	27.58	26.56	26.97	26.42	26.27	27.12

was the case for the garnets, clinopyroxene varies in composition depending on the whole rock chemistry, the metabasites 82244–5 having the more diopsidic composition (X_{Mg} = 0.68–0.70) and the rest of the gabbroic types having X_{Mg} from 0.41 to 0.64 (Fig. 4). In samples 71300 and 96896 (Table 3), the clinopyroxenes included in garnet contain greater Na and Al contents than those in the matrix and also than those in the rest of the sample. The jadeite component in these inclusions varies from 1.0 to 20.5 mol.%, some of the clinopyroxenes thus plotting in the omphacite field in Fig. 4. Omphacite relics are restricted to primary inclusions in garnet. They are absent from the granoblastic matrix. Clinopyroxene included in garnet in sample 96895 has lower Na contents and Mg/(Fe+Mg) ratios than that in the matrix (Fig. 4). Similar relict parageneses have been found in the matrix of eclogites from the Czech Republic (Medaris *et al.*, 1995) where they have been interpreted as representing retrograded eclogitic stages.

Orthopyroxene

Orthopyroxene has been found only in some samples of the Tenzuela massif. Orthopyroxenes have compositions of ~X_{Mg} = 0.29–0.38 in sample 96896 and X_{Mg} = 0.37–0.43 in sample 96895, their chemical composition being controlled by the whole-rock chemistry. Although they appear as inclusions in the garnet they are more abundant in the matrix. Sometimes orthopyroxene appears to be associated with plagioclase and amphibole around garnet, suggesting its involvement in garnet breakdown reactions as discussed below (Fig. 2*e*). No important chemical differences have been found between the different textural types, with the exception of slightly higher Al_2O_3 contents in orthopyroxene included in garnet (up to 1.1 wt.%, Table 3).

Amphibole

Structural formulae have been calculated to 13 cations excluding Ca, Na and K; Fe^{3+} has been

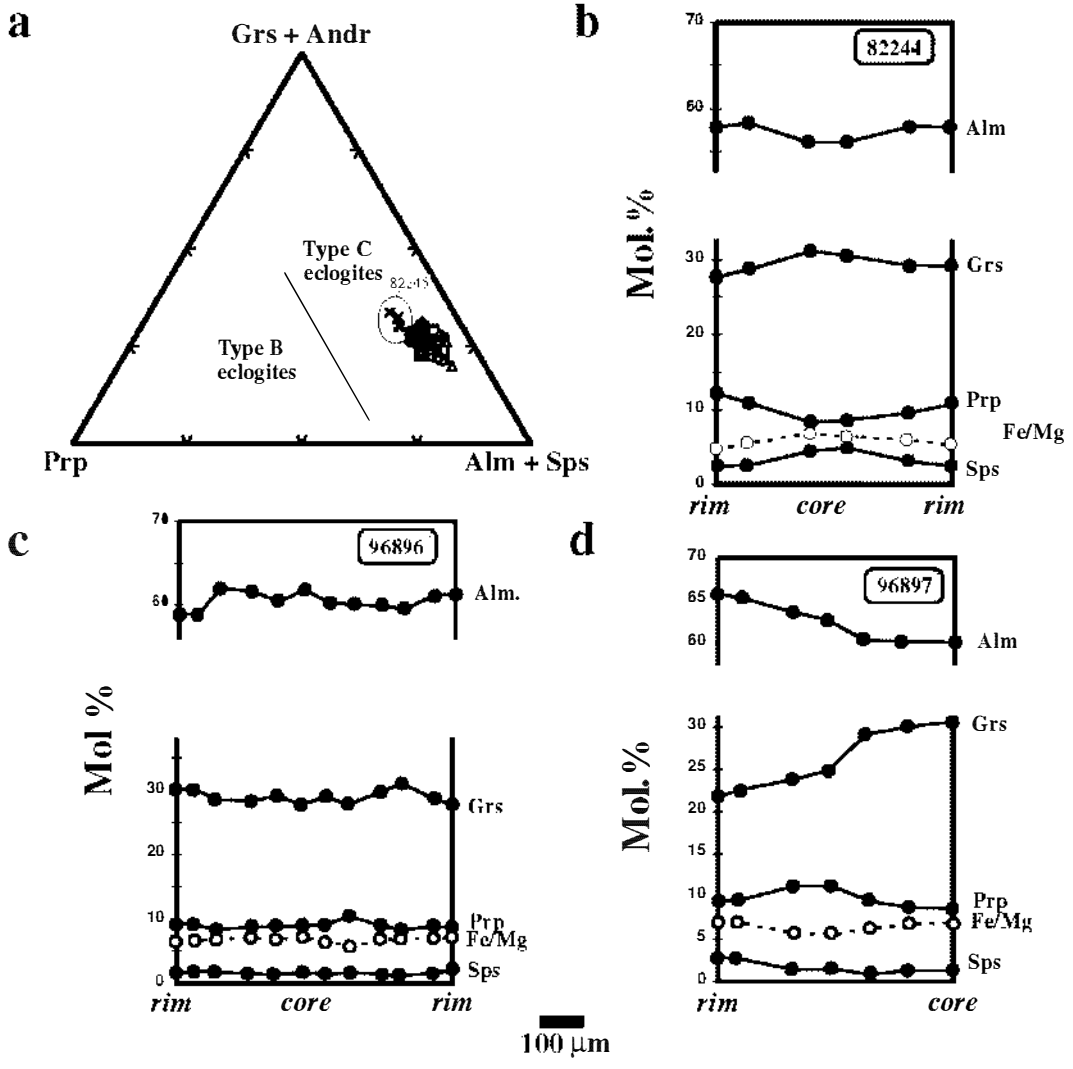

FIG. 3. (*a*) Garnet composition plot in the Prp-(Grs+Andr)-(Alm+Sps) diagram. Note the more calcic composition of the garnets in sample 82245. Fields of type B and C eclogites after Coleman *et al.* (1965). (*b*) Typical unzoned garnet profile in sample 96896. (*c,d*) Zoning profiles with an increase in Fe accompanied by a decrease in Ca from core to rim indicating a down pressure re-equilibration.

calculated according to Robinson *et al.* (1982) and the amphiboles are classified according to Leake *et al.* (1997), (Table 4). All analysed amphiboles are calcic types varying from hastingsite to ferropargasite in the most basic types and from magnesiohastingsite to pargasite and edenite in the most evolved metagabbros (Fig. 5, samples 82244-5). Generally, the amphiboles included in garnet tend to show more magnesian compositions when compared to those in the matrix (Fig. 5). This could be the result of local re-equilibration due to the large volume differences between the host garnet and the amphibole inclusion as stated by Spear (1991) for biotite inclusions in garnet from metapelitic rocks. The amphiboles included in garnet display a slightly higher Al content in comparison with those of the matrix (Fig. 5). This tendency is reflecting progressive down-pressure amphibole recrystallization as will be discussed below. No significant

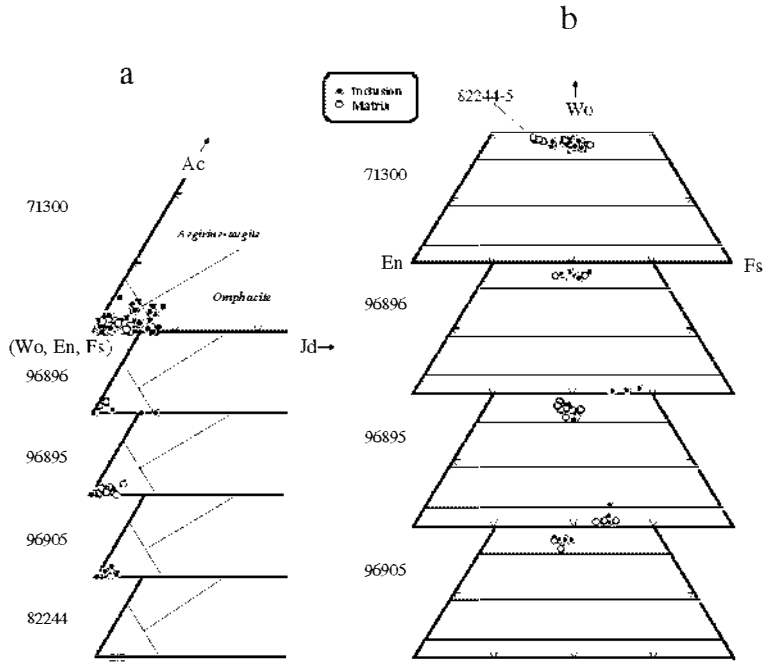

FIG. 4. (*a*) Clinopyroxene composition in terms of jadeite-aegirine-Q(di, en, fs); in samples 71300 and 96896 some clinopyroxene inclusions plot in the field of omphacite. (*b*) wollastonite-enstatite-ferrosilite classification diagram for clino- and orthopyroxenes.

chemical variation has been found in amphibole composition irrespective of its location in relation to garnet domains. When comparing the amphibole composition with that of other amphiboles from different metamorphic regimes we note that they plot in the field of intermediate pressure terrains (Fig. 5). This points to a retrogression during intermediate to lower pressure conditions as is common in other Hercynian eclogites (Messiga *et al.*, 1992; Medaris *et al.*, 1995).

Plagioclase

Most of the plagioclase is found defining coronas around garnet, thus suggesting a post-eclogitic character (Fig. 2). Nevertheless, three textural types of plagioclase were distinguished: inclusions, coronas and matrix. Plagioclase presents similar compositions from sample to sample but in certain cases a wide range of variation within individual rocks occurs. In general, plagioclase composition varies from An_{10} to An_{50} the average being An_{20}. The orthoclase content never exceeds 1 mol.%. In gabbroic sample 71300, the plagioclase included in garnet showed the highest albite content but nevertheless, its composition varies within a narrow range (An_{10} to An_{22}). In contrast, sample 96895 shows plagioclase with a wide compositional variation (An_{50} to An_{10}), the most calcic being that included in garnet. In the last two cases, plagioclase inclusions are the result of the retrograde reaction between eclogitic garnet and clinopyroxene as evidenced by the presence of residual clinopyroxene surrounded by plagioclase coronas inside the garnet (see Fig. 2*d*). In two samples, a compositional profile from the contact with the garnet towards the amphibolitic matrix has been performed, the plagioclase being An_{45} against garnet and An_{28} towards the matrix. This coincides with the decrease in grossular component in the garnet rims, thus confirming the down-pressure re-equilibrium between garnet rims and adjacent plagioclase. This high An content of plagioclase between garnet and amphibole has been observed in other Hercynian retrocclogites (O'Brien *et al.*, 1992).

In every sample, plagioclase in the matrix presents similar compositions to the plagioclases

TABLE 3. Selected clinopyroxene and orthopyroxene analyses from tholeiitic metabasites from the Sierra de Guadarrama.

	Clinopyroxene													Orthopyroxene					
Sample	71300	71300	71300	71300	71300	71300	96895	96895	96895	96895	96896	96896	96896	96895	96895	96896	96896	96896	96896
Texture	incl.	incl.	incl.	incl.	matrix	matrix	incl.	incl.	matrix	matrix	incl.	incl.	matrix			incl.	incl.		
Analysis	61	62	105 (c3)	92	101	105	53	54	79	28	154	162	151	45	34	38	39	140	130
SiO_2	50.65	51.01	52.24	51.80	50.90	49.93	50.40	50.76	52.02	51.47	52.84	50.66	50.42	49.60	50.04	50.55	50.44	48.51	49.22
TiO_2	0.43	0.33	0.33	0.31	0.13	0.08	0.27	0.26	0.08	0.14	0.10	0.03	0.12	0.05	0.03	0.00	0.00	0.11	0.06
Al_2O_3	5.37	5.26	4.88	5.30	3.54	2.02	2.04	1.50	2.70	3.84	6.82	7.00	0.86	0.42	0.42	0.43	0.24	0.40	0.42
FeO	14.93	14.73	14.68	15.22	14.81	19.72	16.77	14.76	14.35	12.00	11.93	15.45	18.18	36.74	35.36	36.33	36.08	39.06	37.88
MnO	0.16	0.23	0.13	0.00	0.08	0.00	0.26	0.21	0.04	0.14	0.22	0.35	0.40	0.59	0.52	0.41	0.53	1.03	0.80
MgO	7.23	7.30	7.49	6.88	9.46	7.23	8.60	9.96	10.06	10.03	7.44	5.99	7.87	12.37	11.56	12.21	12.37	9.15	10.62
CaO	17.71	17.35	17.90	18.95	21.48	21.04	21.43	21.98	20.32	20.04	17.75	18.17	21.13	0.64	0.86	0.62	0.58	0.96	0.70
Na_2O	2.77	2.90	2.48	2.59	0.81	0.65	0.29	0.04	1.05	1.67	2.66	1.98	0.46	0.00	0.02	0.11	0.00	0.00	0.03
Total	99.33	99.18	100.12	101.05	101.24	100.67	100.08	99.52	100.64	99.34	99.83	99.66	99.50	100.60	98.85	100.73	100.28	99.21	99.73
Structural formula O = 6																			
Si	1.93	1.94	1.97	1.94	1.91	1.93	1.95	1.96	1.96	1.94	1.97	1.93	1.97	1.97	2.00	2.00	2.00	1.99	1.99
Al^{IV}	0.07	0.06	0.03	0.06	0.09	0.07	0.05	0.04	0.04	0.06	0.03	0.07	0.03	0.02	0.00	0.00	0.00	0.01	0.01
Ti	0.01	0.01	0.01	0.01	0.00	0.00	0.01	0.01	0.00	0.00	0.00	0.00	0.00	0.00	0.00	0.00	0.00	0.00	0.00
Al^{VI}	0.17	0.18	0.19	0.18	0.07	0.02	0.04	0.02	0.08	0.11	0.27	0.25	0.01	0.00	0.02	0.02	0.01	0.01	0.01
Fe^{3+}	0.08	0.08	0.00	0.05	0.07	0.09	0.02	0.01	0.03	0.06	0.00	0.00	0.05	0.05	0.00	0.00	0.00	0.00	0.00
Fe^{2+}	0.40	0.40	0.46	0.43	0.40	0.55	0.52	0.47	0.42	0.32	0.37	0.49	0.55	1.18	1.19	1.20	1.20	1.34	1.28
Mn^{2+}	0.01	0.01	0.00	0.00	0.00	0.00	0.01	0.01	0.00	0.00	0.01	0.01	0.01	0.02	0.02	0.01	0.02	0.04	0.03
Mg	0.41	0.41	0.42	0.39	0.53	0.42	0.49	0.57	0.56	0.56	0.41	0.34	0.46	0.73	0.69	0.72	0.73	0.56	0.64
Ca	0.72	0.71	0.72	0.76	0.87	0.87	0.89	0.91	0.82	0.81	0.71	0.74	0.88	0.03	0.04	0.03	0.02	0.04	0.03
Na	0.20	0.21	0.18	0.19	0.06	0.05	0.02	0.00	0.08	0.12	0.19	0.15	0.03	0.00	0.00	0.01	0.00	0.00	0.00
End-members																			
QUAD	78.90	78.01	81.62	80.74	93.80	94.99	97.78	99.69	92.19	87.42	79.51	84.35	96.44						
Jd	14.16	15.44	18.38	15.14	3.17	1.01	1.38	0.22	5.54	8.44	20.49	15.65	0.60						
Aegirine	6.94	6.55	0.00	4.12	3.02	3.99	0.84	0.09	2.27	4.15	0.00	0.00	2.96						
En														36.54	35.77	36.71	37.11	28.31	32.35
Fs														62.11	62.31	61.95	61.95	69.56	66.11
Wo														1.36	1.92	1.34	1.34	2.14	1.54

TABLE 4. Selected amphibole analyses of tholeiitic metabasites from the Sierra de Guadarrama.

Sample	71300	71300	71300	71300	71300	96895	96895	96897	96897	96987
Text			Corona	Inclusion	Inclusion					Inclusion
Analysis	4	25	17	24	116	14	65	72	107	108
SiO_2	43.27	40.10	40.28	40.58	40.36	42.96	42.06	44.79	43.47	43.12
TiO_2	1.91	1.35	1.23	1.01	1.98	0.82	0.10	1.19	1.04	0.52
Al_2O_3	9.24	13.75	12.05	13.61	12.42	13.69	13.03	9.04	10.60	11.20
FeO	17.96	20.40	21.85	20.84	23.27	18.58	23.81	19.60	20.91	20.52
MnO	0.00	0.24	0.20	0.14	0.24	0.19	0.64	0.24	0.19	0.14
MgO	10.57	7.23	7.16	7.10	5.92	7.08	5.30	9.02	7.93	8.01
CaO	10.71	11.44	10.91	10.58	9.62	10.49	11.71	10.81	11.06	11.28
Na_2O	2.69	2.99	3.00	3.24	3.05	2.37	0.24	1.88	2.14	1.98
K_2O	0.14	0.23	0.00	0.00	0.18	0.14	0.09	0.05	0.03	0.04
Total	96.49	97.73	96.68	97.09	97.03	96.32	96.98	96.63	97.35	96.81
Structural formula 13-CNK										
TSi	6.51	6.11	6.20	6.17	6.18	6.50	6.37	6.74	6.56	6.52
TAl	1.49	1.89	1.80	1.83	1.82	1.50	1.63	1.26	1.44	1.48
Total T	8.00	8.00	8.00	8.00	8.00	8.00	8.00	8.00	8.00	8.00
CAl	0.15	0.57	0.38	0.61	0.41	0.94	0.69	0.34	0.44	0.52
CFe^{3+}	0.00	0.35	0.00	0.00	0.86	0.26	1.03	0.60	0.57	0.59
CTi	0.22	0.15	0.14	0.12	0.23	0.09	0.01	0.13	0.12	0.06
CMg	2.37	1.64	1.64	1.61	1.35	1.60	1.20	2.02	1.78	1.81
CFe^{2+}	2.26	2.25	2.81	2.65	2.12	2.09	1.99	1.86	2.07	2.00
CMn	0.00	0.03	0.03	0.02	0.03	0.02	0.08	0.03	0.02	0.02
Total C	5.00	5.00	5.00	5.00	5.00	5.00	5.00	5.00	5.00	5.00
BCa	1.73	1.87	1.80	1.72	1.58	1.70	1.90	1.74	1.79	1.83
BNa	0.27	0.13	0.20	0.28	0.42	0.30	0.07	0.26	0.21	0.17
Total B	2.00	2.00	2.00	2.00	2.00	2.00	1.97	2.00	2.00	2.00
ANa	0.51	0.75	0.69	0.68	0.48	0.39	0.00	0.29	0.41	0.41
AK	0.03	0.04	0.00	0.00	0.03	0.03	0.02	0.01	0.00	0.01
Total A	0.54	0.79	0.69	0.68	0.52	0.42	0.02	0.30	0.42	0.42
Total cations	15.54	15.79	15.69	15.68	15.52	15.42	14.99	15.30	15.42	15.42

of the inclusions and coronas. As previously, a tendency towards more calcic composition close to the garnet domain is seen.

Whole-rock chemistry and petrogenesis of the metabasite protoliths

The major and trace elements of nine metabasites are given in Table 5. Three samples are taken from Villaseca (1983) with new trace and *REE* analyses carried out at the CRPG-CNRS (Nancy, France).

The analysed metabasites range in composition from gabbro to leucotonalite showing a large degree of differentiation, the most variable types being those cropping out at Tenzuela massif (Fig. 1) (Villaseca, 1983). In other outcrops the metagabbroic composition dominates. The CIPW normative compositions range from olivine-normative (<15 wt.%) in the gabbros towards quartz-normative for rocks with SiO_2 contents of >49 wt.%. The metabasic series vary from silica saturated to oversaturated. The most differentiated rock (leucotonalite 67041, Table 5) has up to 0.51 wt.% normative corundum. The subalkaline chemical composition together with their very low K_2O content defines a tholeiitic affinity for these metabasites. This tholeiitic character is also

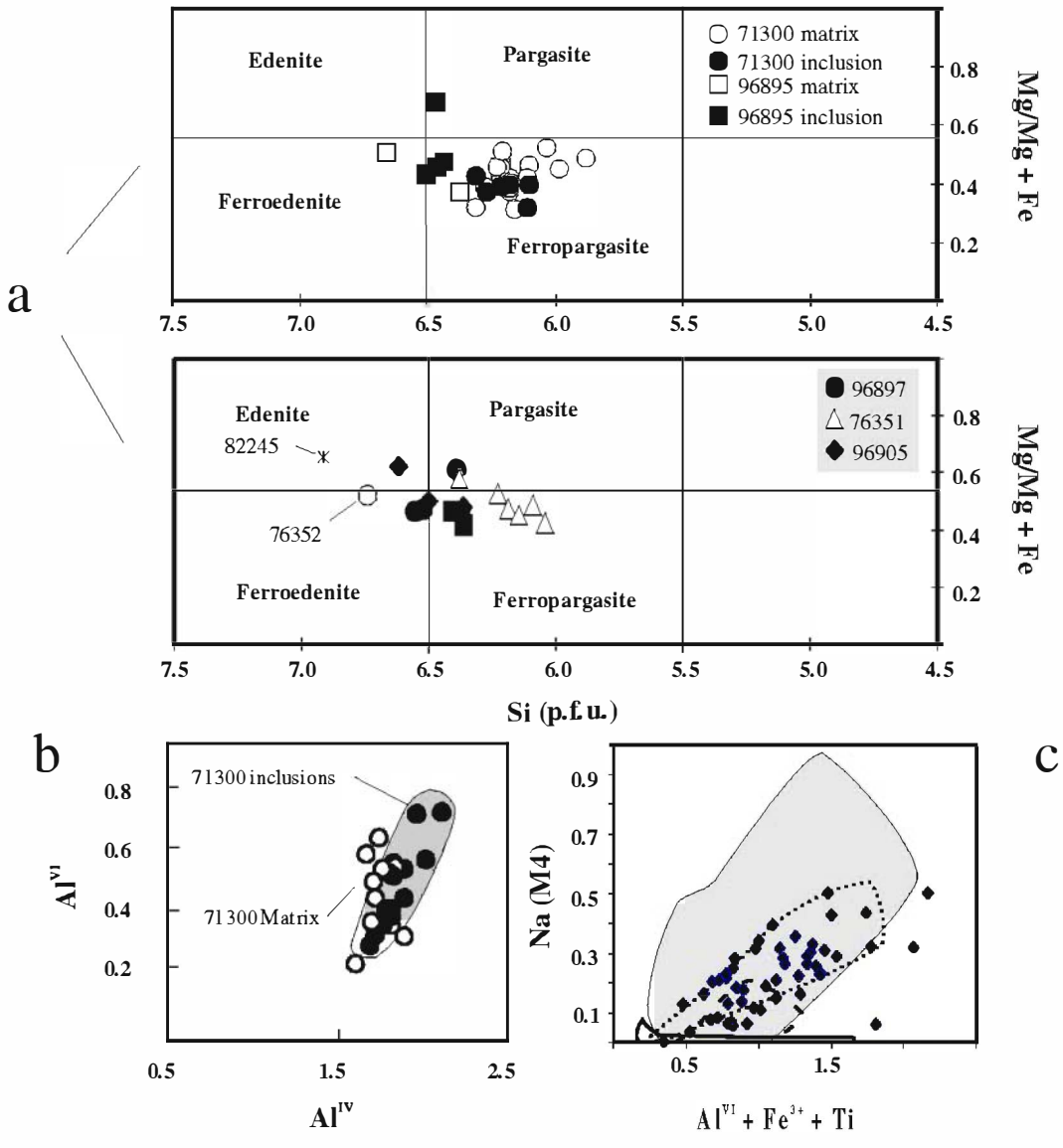

FIG. 5. (*a*) Composition of Ca-amphiboles from the Central Spain metabasites (Leake *et al.*, 1997); (*b*) concentration of Al in four and six fold coordinates sites for inclusion and matrix amphiboles of sample 71300; (*c*) $Na(M_4)$ *vs.* $Al^{VI}+Fe^{3+}+Ti$ diagram of amphiboles from Central Spain metabasites compared to amphiboles of different metamorphic facies series. Shaded field: Sanbagawa and Franciscan high pressure facies series; dotted line: Dalradian intermediate pressure facies; continuous line: Haast River intermediate pressure facies; dashed line: Abukuma low pressure terrane; from Laird and Albee (1981).

shown by the high Fe content of the metabasites in the AFM diagram (Fig. 6*a*). The P_2O_5 contents are generally high compared to other tholeiitic series. In fact, in the $MnO-TiO_2-P_2O_5$ diagram (Fig. 6*b*) these metabasites plot from tholeiitic towards more alkaline fields (Mullen, 1983).

The HFSE and *REE* are usually regarded as trace elements remaining unaffected by metamorphic processes (Rollinson, 1993). All the analysed metabasites are richer in Th, Nb, Zr and LILE than averaged MORB composition (Fig. 6*c*). In fact, in the Zr/Y *vs.* Zr diagram (not shown),

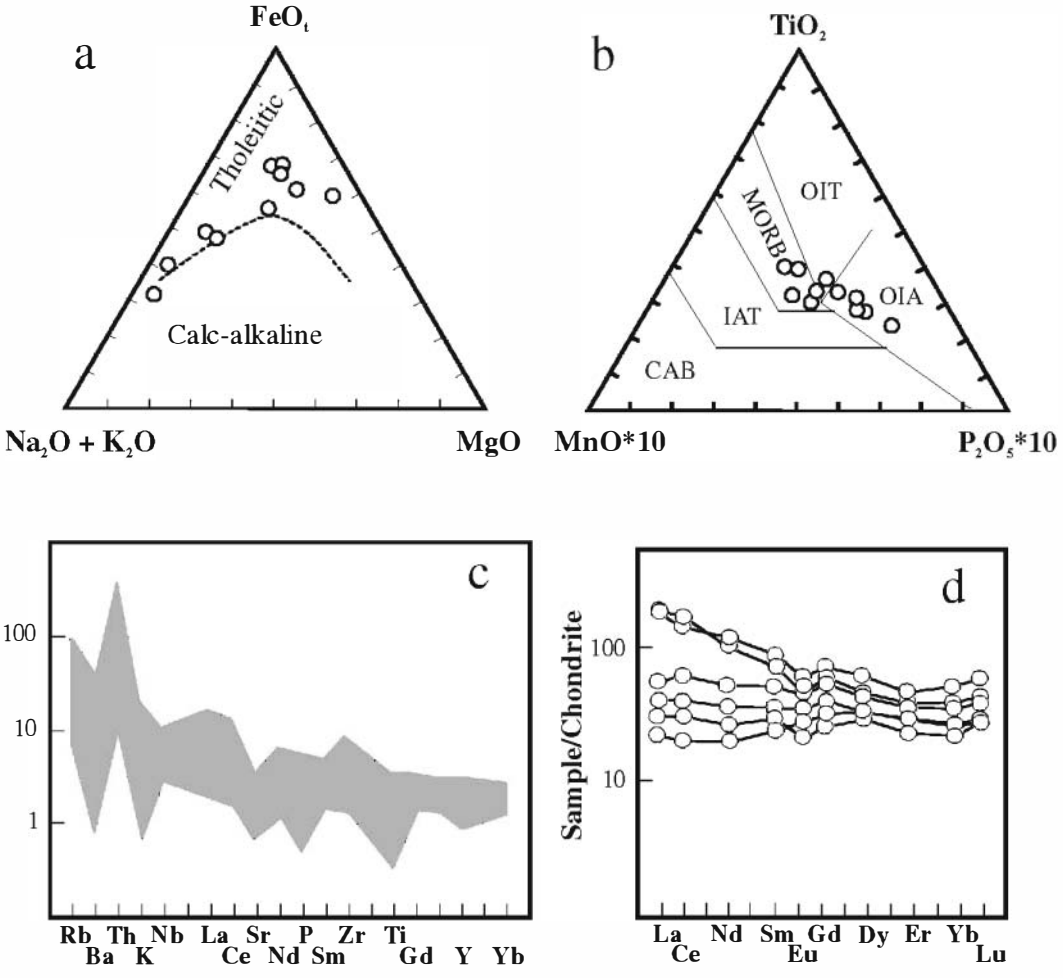

FIG. 6. (*a*) AFM diagram for the Central Spain metabasites showing the typical Fe enrichment of the tholeiitic series; fields after Irvine and Baragar (1971). (*b*) MnO-TiO_2-P_2O_5 discrimination diagram with fields after Mullen (1983). (*c*) N-type MORB (Saunders and Tarney, 1984; Sun, 1980) normalized diagram for metabasites; CAB, island-arc calc-alkaline basalt; IAT, island-arc tholeiite; OIT, ocean-island tholeiite; OIA, ocean-island alkali basalt. (*d*) C1 chondrite (Evensen *et al.*, 1978) normalized *REE* diagram.

these metabasites plot mostly in within-plate fields, far from the composition of oceanic or plate-margin basalts (Pearce and Norry, 1979). Although the metagabbros varieties exhibit flat chondrite-normalized *REE* patterns (La_N/Yb_N = 1.0–1.8) they show absolute concentrations of ~20 times chondrite (Fig. 6*d*). The more silica-rich metabasites display *LREE*-enriched patterns (La_N/Yb_N = 3.6) and some negative Eu anomaly, but *HREE* patterns are consistently flat suggesting that neither garnet nor amphibole were important phases involved in the petrogenesis of the tholeiites.

In summary, we believe that the metabasic protolith derived from low-pressure crystal fractionation of tholeiitic melts more enriched than typical MORB compositions. Their association with typical continental platform sediments such as mature pelites, calc-silicates, marbles and minor quarzites, defines a continental affinity and not an oceanic character for these tholeiitic sills. The high degree of evolution acquired by these metabasites is illustrated by the presence of felsic types which is in agreement with intracontinental scenarios proposed by Hess (1989).

TABLE 5. Major and trace element analysis of selected metabasites.

Sample	71300	96895	96896	62984	71303	82244	9512	66726	67056	67041
SiO_2	44.41	46.34	48.23	48.60	49.50	50.43	51.79	63.92	69.44	72.77
TiO_2	4.36	3.81	3.46	2.89	2.22	1.94	1.93	1.28	0.58	0.43
Al_2O_3	13.02	12.82	13.12	14.73	13.59	13.43	14.14	14.11	13.68	14.36
Fe_2O_3	20.11	18.66	17.75	13.38	14.08	14.51	12.55	7.73	5.28	3.21
MnO	0.40	0.31	0.28	0.22	0.27	0.23	0.22	0.08	0.04	0.03
MgO	4.36	4.77	4.19	4.88	7.52	5.43	6.42	1.37	0.66	0.62
CaO	9.51	9.54	8.95	8.13	10.53	10.64	10.50	4.64	3.3	2.43
Na_2O	3.56	3.33	3.39	3.53	1.27	2.94	1.70	5.72	5.08	5.49
K_2O	0.43	0.15	0.36	1.46	0.24	0.05	0.31	0.43	1.46	0.51
P_2O_5	0.32	0.45	0.52	0.64	0.26	0.12	0.25	0.29	0.2	0.06
LOI	0.90	0	0	1.50	1.23	0.39	0.46	0.22	0.22	0.4
Total	101.38	99.92	99.95	99.96	100.71	100.41	100.27	99.79	99.94	100.31
Ba	123	25	67	129	241	28		117	224	123
Rb	10	4	15	54	5	9		12	30	12
Sr	61	62	76	136	87	109		141	122	324
Nb	15	12	15			7		24	20	
Zr	154	191	241	190	100	102		541	665	564
Y	42	50	63		25	40		91	74	53
Th	5	1.3	1.84		17	4		14	15	
Ga	29	22	24	24		21		27	26	
La	4.91	9.06	13.04			7.09		39.70	41.72	
Ce	12.23	23.01	36.66			17.72		83.77	98.07	
Nd	8.79	16.33	24.61			11.89		50.18	45.78	
Sm	3.78	5.25	7.9			4.43		13.28	11.37	
Eu	1.55	1.8	2.52			1.23		3.36	2.22	
Gd	6.46	7.52	9.59			5.20		12.96	11.13	
Dy	8.28	8.32	10.96			6.22		14.58	11.46	
Er	3.76	4.8	6.14			3.33		7.55	6.86	
Yb	3.89	4.51	5.88			3.73		8.70	6.66	
Lu	0.68	0.74	0.93			0.67		1.46	1.05	

P-T conditions

For kinetic reasons, mafic rocks tend to preserve high-pressure parageneses relative to felsic rocks (O'Brien *et al.*, 1992). The presence of scarce omphacitic pyroxene included in garnet in certain samples indicates that the *P-T* evolution of these rocks passed through a high *P* stage.

M_2 granulitic re-crystallization is proven by the presence of plagioclase coronas around clinopyroxene inclusions in garnet (Fig. 2). This indicates the occurrence of the reaction:

$$\text{Grt} + \text{Omp} \rightarrow \text{Pl}\ (<\text{An}) + \text{Cpx}\ (\text{low Na}) \quad (1)$$

instead of reactions involving quartz (e.g. GADS, O'Brien *et al.*, 1992) as these metagabbros present an olivine-normative composition.

Reaction 1 marks the transition from eclogite to granulite facies conditions.

The widespread presence of plagioclase and pargasitic amphibole coronas around garnet and the general amphibolitization of the rock (Fig. 2) as H_2O pressure increases are controlled by reactions such as:

$$\text{Grt} + \text{Cpx} \rightarrow \text{Pl}\ (>\text{An}) + \text{Amp} \quad (2)$$

(Spear, 1993) which is also typical of the M_2 metamorphic re-crystallization episode. The local presence of orthopyroxene in the inner coronas around garnet (Fig. 2*e*) indicates a reaction of the form

$$\text{Grt} + \text{Cpx}\ (\pm\text{Qtz}) \rightarrow \text{Opx} + \text{Pl} \quad (3)$$

which is less common than reaction 2 probably

because of minor variations in the whole-rock composition of the metabasites and/or the presence of minor volatile phases during the eclogite retrogression. The last two reactions are probably coupled because: (1) the outer amphibole-rich rim is concentric to the orthpyroxene + plagioclase inner rim (Fig. 2*e*); and (2) both the orthopyroxene and the amphibole were formed during granulitic conditions as deduced from the *P-T* estimates as discussed below.

This metamorphic evolution is represented in terms of ACF diagrams in Fig. 7. The tie-lines connecting Jd-rich clinopyroxene and garnet (eclogite paragenesis) switch to a new tie-line connecting Ca-rich plagioclase and amphibole (reaction 2), and Na-rich plagioclase and diopsidic clinopyroxene (reaction 1). In certain microdomains of some metagabbros (sample 96895, Fig. 7) reaction 3 can take place together with reaction 2 with the new orthopyroxene–plagioclase assemblage formed in the inner zones towards the garnet (Fig. 2).

The peak pressure eclogitic conditions are documented by the paragenesis Alm-Grs-Prp garnet + omphacite + rutile + quartz.

Combination of the garnet-clinopyroxene Fe-Mg exchange thermometer (Ellis and Green, 1979; Krogh, 1988) and the geobarometer based on the reaction: albite in plagioclase = jadeite (in omphacite) + quartz (Holland, 1980) yields pressure-temperature conditions (Fig. 8) of ~14 ± 2 kbar and 700 ± 50°C (sample 71300), 12 ± 2 kbar and 675 ± 50°C (sample 82244). Inclusion omphacite and adjacent core garnet were used in all cases.

Pressure-temperature estimates have also been made using TWEEQU techniques as described by Berman (1991) using the end-member properties and thermodynamic database of Berman (1988; 1990). The solution models used in the calculations are from Berman (1990) for garnet; Fuhrman and Lindsley (1988) for plagioclase, and ideal models are used for pyroxenes. Reaction curves were calculated for the mineral compositions given in Tables 2–4 and the assemblages deduced from petrographic studies (Table 1) considered to be representative of the first Hercynian metamorphic episode. Intersections giving standard deviations of ±0.5 bar and ±20°C after no more than one iteration in the exclusion analysis are regarded as yielding acceptable results. Core-inclusions representing peak pressure conditions and border and matrix phases representative of the later retrogression stages are treated separately.

The eclogite–granulite transition paragenesis in sample 71300 with omphacitic pyroxene inclusions in garnet, produce a tight crossing of reactions (two independent) at pressures of ~14 kbar and temperatures of ~760°C (Fig. 9). This is considered to represent the highest pressure attained in the area. Similar *P-T* values are obtained, nevertheless, for other samples like 76352, 82244 and 96895 for equilibrium parageneses Grt + Pl + Cpx + Qtz + Ilm + Rt resulting in tight crossing of all equilibria (two independent) as illustrated in Fig. 9.

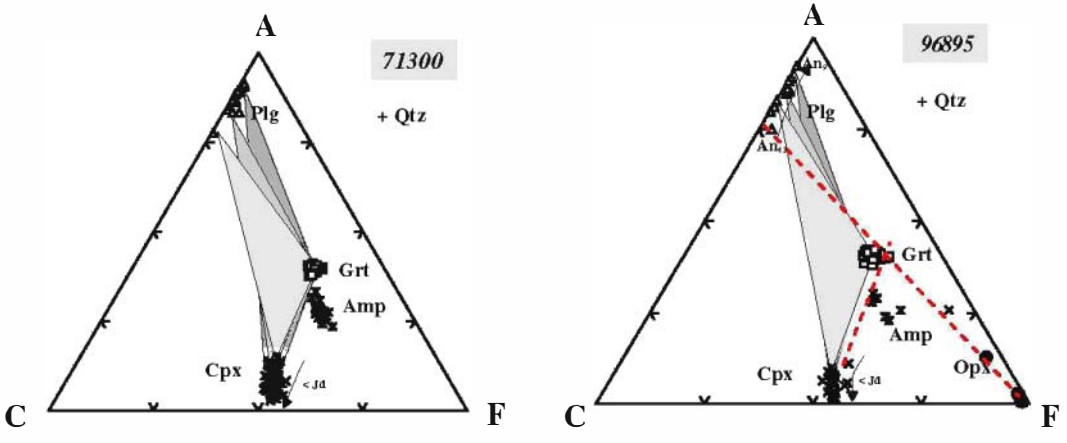

FIG. 7. ACF diagrams showing the tie-line switching from gnt-cpx (jd rich) assemblages toward a typical granulite facies paragenesis with plagioclase and amphibole and/or orthopyroxene.

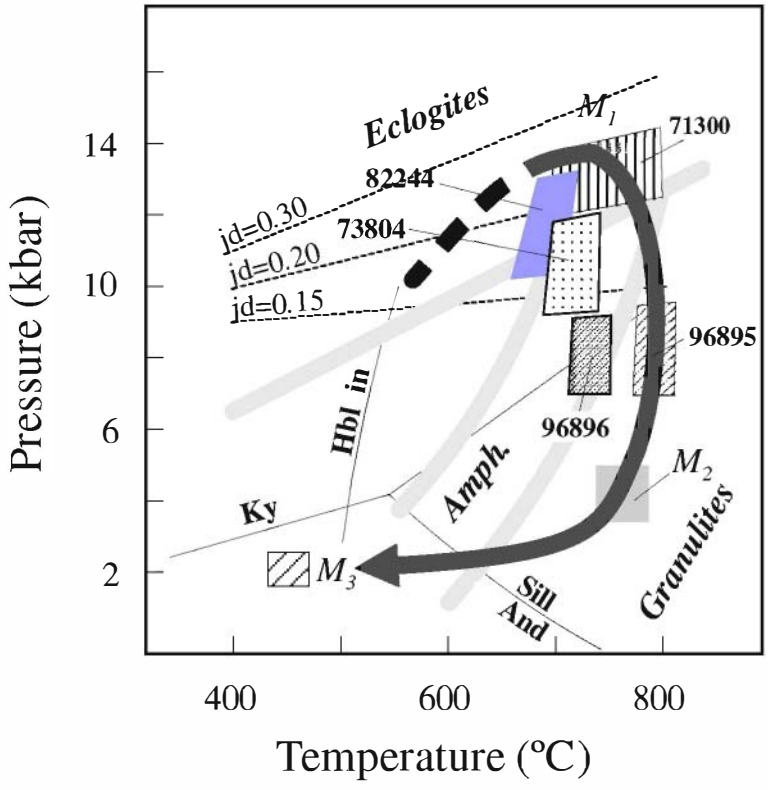

FIG. 8. *PT* diagram in which the results of several classical thermobarometers in different samples (textured quadrangular areas with respective sample number) for the M_1 and M_2 metamorphic stages are shown. M_2 peak conditions from Martín Romera *et al.* (1999). M_3 metamorphic conditions from Villaseca (1983) and Arenas *et al.*, (1991). Thick grey arrow shows a possible *PT* metamorphic path for the Sierra de Guadarrama sector as deduced from the metamorphic conditions of the three main metamorphic stages. Jadeite isopleths are after Gasparik and Lindsley (1980); Hbl in reaction after Winkler (1976); Ky-And-Sill is after Holdaway (1971); facies boundaries drawn after Spear (1993).

Relics of high-pressure M_1 assemblages in the related layered metasedimentary sequence have also been identified (Villaseca, 1983; Villaseca and Barbero, 1994). These relics consist of kyanite, Mg-rich garnet (Alm_{63}-Pir_{33}-$Gros_3$-Sps_1), rutile and occasional staurolite from which pressure estimates of ~8–15 kbar for temperatures of 700±25°C have been reported (Villaseca and Barbero, 1994). So, the similarity of *P-T* conditions deduced for the M_1 stage for both the paragneisses and the related metabasites indicates that the whole complex has experienced the same burial history.

In metabasites with well-developed plagioclase coronas around garnet, it is possible to estimate core and rim conditions and a record of the two main re-crystallization episodes M_1 and M_2 is obtained. For example, calculations performed on sample 82244, for the equilibrium parageneses Grt + Pl + Cpx + Qtz + Ilm + Rt with garnet core composition and Cpx, Plg, Ilm and Rt inclusions produce tight crossing of all equilibria at pressures in the range of 12–13 kbar and *T* in the range 700 to 750°C. Results in the same sample for garnet rim compositions and matrix phases give *P-T* conditions of 8 kbar at temperatures of ~700°C. Similar decompressional *P-T* paths are obtained for other samples thus confirming the validity of these calculations (Figs 8, 9). Temperature conditions obtained for the M_2 episode, without taking amphibole into account in the calculations, are consistent with those deduced from the conventional garnet-amphibole thermometer (Graham and Powell,

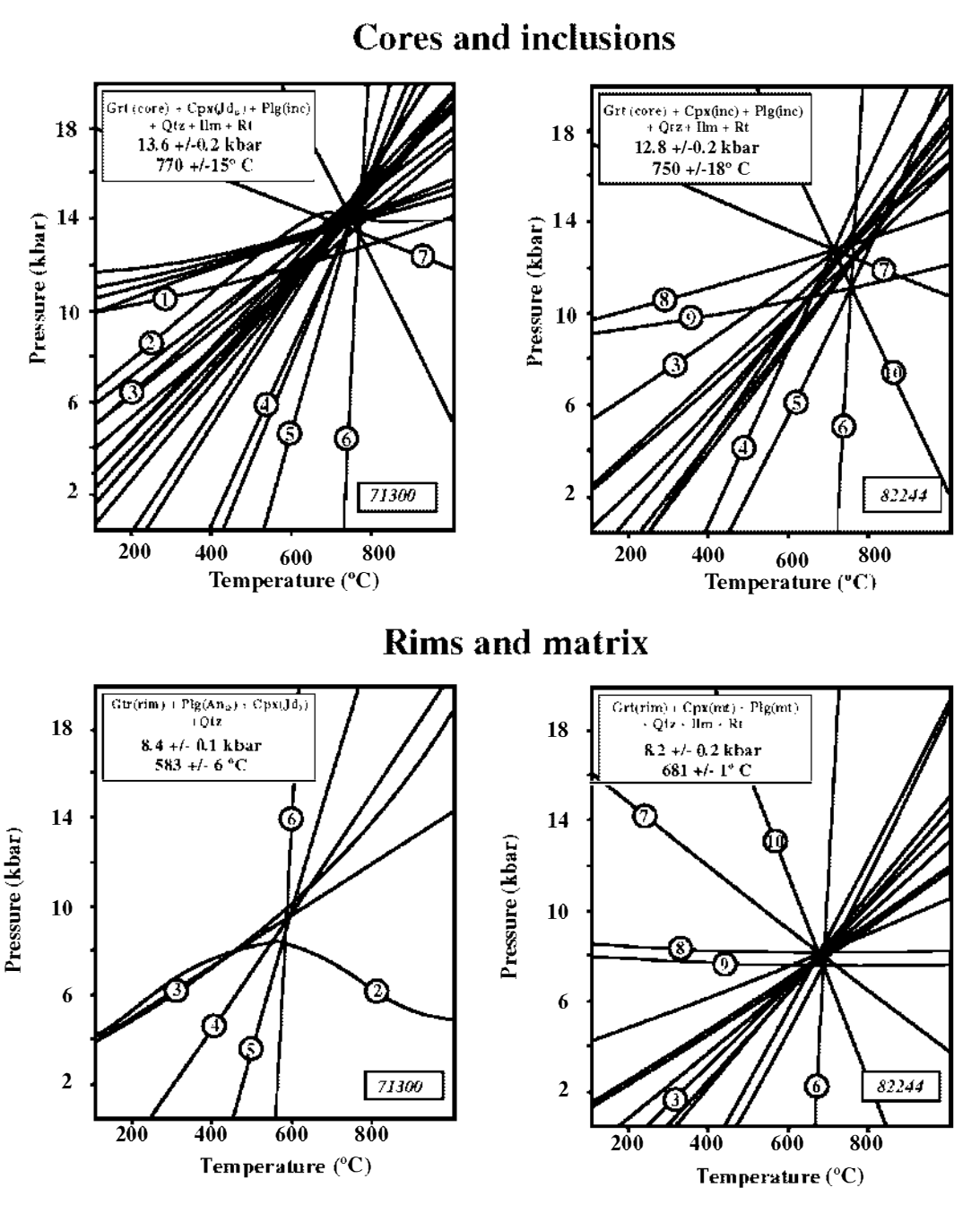

FIG. 9. *PT* estimates based on the TWQ intersections for cores-inclusions and rims-matrix of individual samples using the mineral assemblages shown in the insets and some of the reactions (labelled) of the Appendix. See text for further details of the activity models used, thermodynamic data set and uncertainties of the intersections.

1984) which give results in the range 680 to 750°C. Similar results are obtained using the two pyroxene thermometer from Wood and Banno (1973) considering matrix phases (800–850°C in sample 96895, 750–800°C in sample 96896) and also with the garnet-orthopyroxene geothermometer from Harley (1984) considering garnet rims and adjacent matrix orthopyroxene (760–800°C, sample 96896). Pressures during the M_2 episode must be <7–8 kbar as the jadeite component in clinopyroxene is always <10% (Fig. 8) which is consistent with the results obtained using the internally consistent thermodynamic database as discussed above.

The related paragneisses enclosing the eclogitic metabasic lenses evolve cofacially with them, displaying K-feldspar, biotite, cordierite, and sillimanite as part of a decompressive M_2 paragenesis, whose path must clearly cross into the sillimanite stability field (Fig. 8). Thermobarometric estimates based on garnet – biotite and GASP equilibria give T in the range 740–780°C and P of 4–6 kbar (Martín Romera *et al.*, 1999), which is in agreement with the granulitic peak conditions estimated in the metabasites.

Discussion

High-pressure mineral assemblages reflecting the peak pressure conditions in rocks from the axial Hercynian sectors are remarkably scarce. In the Hercynides from central Spain, the main remains of a high-pressure event are the rare omphacitic pyroxenes included in garnet described in this and previous works (Villaseca, 1983; Villaseca and Barbero, 1994). The first Hercynian tectonometamorphic phase recorded in the Spanish Central System is Devonian in age, and is marked by the interruption of Palaeozoic sedimentation (Gutiérrez Marcos *et al.*, 1990). In coincidence with this assumption are the ages of 370–380 Ma which Wildberg *et al.*, (1989) obtained from zircon from different paragneisses and orthogneisses from the eastern part of the Sierra de Guadarrama and which they assume reflect the first Hercynian compressive event (D_1).

The metamorphic climax with associated crustal anatexis is estimated to have occurred at ~325–330 Ma based on geochronological data such as U-Pb in monazite from gneisses of the eastern part of the Sierra de Guadarrama (Valverde Vaquero *et al.*, 1995; Escuder Viruete *et al.*, 1998).

Peak pressure conditions based on the eclogitic relics in the metabasites studied in this work are estimated to be ~14 kbar and 750°C. Pressure-temperature estimates made on garnet rims and matrix phases vary from 6 to 10 kbar and 680 to 800°C. As the metamorphic climax conditions of the area have been estimated to be at even lower pressures (4–6 kbar, Villaseca, 1983), the total decompression range has to be ~8–10 kbar (Fig. 8). The *P-T* path thus obtained shows an isothermal decompression, and in any case, an important increase in temperature related to thermal relaxation is not observed. Such an isothermal decompression requires unroofing of deep-placed metamorphic rock to be rapid compared to the rate of thermal relaxation and subsequent cooling, but not so rapid as to preserve abundant high-pressure relics. Whether the exhumation is related to extension of an overthickened and /or thermally weakened orogenic crust (Ridley, 1989; Ruppel and Hodges, 1994) or thrusting accomplished by high rates of synorogenic erosion (Jamieson *et al.*, 1995; Willett *et al.*, 1993), or a combination of the two, is a difficult question to answer with the present data. Nevertheless, the presence of a system of extensional detachments such as the Berzosa-Riaza shear zones in the Sierra de Guadarra, (Escuder Viruete *et al.*, 1998) suggests that the near isothermal decompression path could be largely controlled by these extensional tectonics. Relatively rapid extrusion uplift permits the transition from the eclogite field to the sillimanite stability field. Isostatic erosion (England and Thompson, 1984) never reaches such a large-scale advection of heat and the *P-T* path never reaches the sillimanite field (Thompson *et al.*, 1997). With the geochronological data available, this decompression has occurred during a time span of ~40–50 Ma.

It is remarkable that these high-pressure metamorphic rocks occur in an intracontinental section of the Hercynian orogen, implying a large thickening of the continental crust during the Hercynian collision. The new barometric estimates made in this work allow us to envisage a burial depth for these metabasites of ~55 km (considering an average density for the crust in this sector of ~2.7 g cm^{-3}). Taking into account that there is no evidence of important tectonic imbrication of different crustal slices since Hercynian times, and that the present thickness of the crust in Central Spain is ~31 km (Paulssen and Visser, 1993) the Hercynian crust during the

M_1 stage could have reached a thickness of ~70–80 km, which is more than the double the present thickness. This has important consequences when modelling the Hercynian tectonothermal evolution in the Central Iberian Zone, as the crustal thickening is a major factor controlling melting conditions during orogenesis (Patiño Douce and Johnston, 1991).

Eclogites described in other Hercynian Iberian sectors have been related to eo-Hercynian (430–365 Ma) subduction processes of continental wedges under oceanic crust as in the case of eclogites from the northwest branch (Martínez Catalán *et al.*, 1996) or southwestern sectors (Leal *et al.*, 1996). These eclogites are incorporated tectonically into major allochthonous-parautochthonous units and are closely related to mantle-derived peridotitic bodies, as is also typical in most of the European Hercynian eclogite-facies rocks (Carswell and Cuthbert, 1986; Bouchardon *et al.*, 1989). In contrast, the eclogite-facies metabasites studied in the present work do not show any relationship with ultramafic mantle-derived rocks and lack a geochemical oceanic affinity, their chemical features being consistent with an intraplate continental affinity. The absence of tectonic contacts between the metabasites and host rock and the cofacial metamorphic evolution argues against any suggestion that the host rocks have never endured such high pressure conditions because they came into contact with the eclogites much later at some shallower depth. Thus is seems reasonable to state that no differences in metamorphic grade exist between the metabasites and the host rocks, the metabasites having suffered *in situ* eclogite-facies metamorphism and thus do not represent allochthonous units. Burial of the whole metamorphic sequence and subsequent eclogitization of the basic rocks might be related to intracontinental subduction thickening during the Hercynian collision.

Acknowledgements

Alfredo Fernández Larios and José González del Tánago are thanked for their assistance in microprobe analysis performed at CAI of Microscopía Electrónica from Complutense University. F. J. Fernández, P. J. O'Brien and an anonymous reviewer are thanked for their constructive comments. This work was supported financially by the project DGYCIT PB96-0661 of the Spanish Ministerio de Educación y Cultura.

References

Arenas, R., Fúster, J.M., González Lodeiro, F., Macaya, J., Martín-Parra, L.M., Martínez-Catalán, J.R. and Villaseca, C. (1991) Evolución metamórfica de la región de Segovia (Sierra de Guadarrama). *Geogaceta*, **4**, 195–201.

Barbero, L. (1995) Granulite facies metamorphism in the Anatectic Complex of Toledo, Spain: late Hercynian tectonic evolution by crustal extension. *J. Geol. Soc.*, **152**, 365–82.

Berman, R.G. (1988) Internally-consistent thermodynamic data for minerals in the system Na_2O-K_2O-CaO-MgO-FeO-Fe_2O_3-SiO_2-TiO_2-H_2O-CO_2. *J. Petrol.*, **29**, 445–522.

Berman, R.G. (1990) Mixing properties of Ca-Mg-Fe-Mn garnets. *Amer. Mineral.*, **75**, 328–44.

Berman, R.G. (1991) Thermobarometry using multi-equilibrium calculations: a new technique with petrological applications. *Canad. Mineral.*, **29**, 833–55.

Blundy, J.D. and Holland, T.J.B. (1990) Calcic amphibole equilibria and a new amphibole-plagioclase geothermometer. *Contrib. Mineral. Petrol.*, **104**, 208–24.

Bouchardon, J.-L., Santallier, D., Briand, D., Ménot, R.-P. and Piboule, M. (1989) Eclogites in the French Paleozoic Orogen: geodynamic significance. *Tectonophysics*, **169**, 317–32.

Carswell, D.A. and Cuthbert, S.J. (1986) Eclogite facies metamorphism in the lower continental crust. Pp. 193–209 in: *The Nature of the Lower Continental Crust* (J.B. Dawson, D.A. Carswell, J. Hall and K.H. Wedepohl, editors). Spec. Publ., **24**. Geological Society, London.

Coleman, R.G., Lee, D.E., Beatty, L.B. and Brannock, W.W. (1965) Eclogites and eclogites: their differences and similarities. *Geol. Soc. Amer. Bull.*, **76**, 483–508.

Ellis, D.J. and Green, D.H. (1979) An experimental study of the effect of Ca upon garnet-clinopyroxene Fe-Mg exchange equilibria. *Contrib. Mineral. Petrol.*, **71**, 13–22.

England, P.C. and Thompson, A.B. (1984) Pressure-temperature-time paths of regional metamorphism I. Heat transfer during the evolution of regions of thickened continental crust. *J. Petrol.*, **25**, 894–928.

Escuder Viruete, J., Hernáiz, P.P., Valverde-Vaquero, P., Rodriguez Fernández, R. and Dunning, G. (1998) Variscan syncollisional extension in the Iberian Massif: structural, metamorphic and geochronological evidence from the Somosierra sector of the Sierra de Guadarrama (Central Iberian Zone, Spain). *Tectonophysics*, **290**, 87–109.

Evensen, N.M., Hamilton, P.J. and O'Nions, R.K. (1978) Rare earth abundances in chondritic meteorites.

Geochim. Cosmochim. Acta, **42**, 1199–212.

Fuhrman, M.L. and Lindsley, D.H., (1988) Ternary-feldspar modelling and thermometry. *Amer. Mineral.*, **73**, 201–15.

Gasparik, T. and Lindsley, D. (1980) Phase equilibria at high pressure of pyroxenes containing monovalent and trivalent ions. Pp. 309–99 in: *Pyroxenes* (Ch.T. Prewitt, editor). Reviews in Mineralogy, **7**. Mineralogical Society of America, Washington DC.

Govindaraju, K. and Mevelle, G. (1987) Fully automated dissolution and separation methods for the inductively coupled plasma atomic emision spectrometry rock analysis – Application to the determination of rare-earth elements. *J. Anal. Atom. Spectr.*, **2**, 615–21.

Graham, C.M. and Powell, R. (1984) A garnet-hornblende geothermometer: calibration, testing and application to the Pelona Schist, Southern California. *J. Metam. Geol.*, **2**, 13–31.

Gutiérrez Marco, J.C., San José, M.A. and Pieren, A.P. (1990) Central Iberian Zone. Post-Cambrian Paleozoic stratigraphy. Pp. 160–71 in: *Pre-Mesozoic Geology of Iberia* (R.D. Dallmeyer and E. Martínez García, editors). Springer Verlag, Berlin.

Harley, S.L. (1984) An experimental study of the partitioning of Fe and Mg between garnet and orthopyroxene. *Contrib. Mineral. Petrol.*, **86**, 359–73.

Hess, P.C. (1989) *Origins of Igneous Rocks*. Harvard University Press, Cambridge, MA.

Holdaway, M.J. (1971) Stability of andalusite and the aluminium silicate phase diagram. *Amer. J. Sci.*, **27**, 97–132.

Holland, T.J.B. (1980) The reaction albite = jadeite + quartz determined experimentally in the range 600–1200°C. *Amer. Mineral.*, **65**, 129–34.

Irvine, T.N. and Baragar, W.R.A. (1971) A guide to the chemical classification of the common volcanic rocks. *Canad. J. Earth Sci.*, **8**, 523–48.

Jamieson, R.A., Culshaw, N.G. and Corrigan, D. (1995) North-west propagation fo the Grenville orogen: Grenvillian structure and metamorphism near Key Harbour, Georgian Bay, Ontario, Canada. *J. Metam. Geol.*, **13**, 185–207.

Kretz, R. (1983) Symbols for rock forming minerals. *Amer. Mineral.*, **68**, 277–9.

Krogh, E.J. (1988) The garnet-clinopyroxene Fe-Mg geothermometer – a reinterpretation of existing experimental data. *Contrib. Mineral. Petrol.*, **99**, 44–8.

Laird, J. and Albee, A.L. (1981) Pressure-temperatures and time indicators in mafic schists: their application to reconstructing the polymetamorphic history of Vermont. *Amer. J. Sci.*, **281**, 127–75.

Leake, B.E. and 20 others (1997) Nomenclature of amphiboles: Report of the Subcommittee on Amphiboles of the International Mineralogical Association Commission on New Minerals and Mineral Names. *Mineral. Mag.*, **61**, 295–321.

Leal, N., Pedro, J., Moita, P., Fonseca, P., Araújo, A. and Munhá, J. (1996) Metamorfismo nos sectores meridionais da zona de Ossa-Morena: Actualização de conhecimentos. *Estudios sobre a geologia da zona de Ossa-Morena (Maciço Ibérico) Livro Homenagem ao Prof. Francisco Gonçalves, Évora*, 119–32.

Macaya, J., González-Lodeiro, F., Martínez Catalán, J.R. and Álvarez, F. (1991) Continuous deformation, ductile thrusting and backfolding of cover and basement in the Sierra de Guadarrama, Hercynian orogen of central Spain. *Tectonophysics*, **191**, 291–309.

Martínez Catalán, J.R., Arenas, R., Díaz García, F., Rubio Pascual, F.J., Abati, J. and Marquínez, J. (1996) Variscan exhumation of a subducted Paleozoic continental margin: The basal units of the Órdenes Complex, Galicia, NW Spain. *Tectonics*, **15**, 106–21.

Martín Romera, C., Villaseca, C. and Barbero, L. (1999) Materiales anatécticos en el área de Sotosalbos (Segovia, Sierra de Guadarrama). Caracterización petrológica, geoquímica e isotópica (Sr, Nd). *Actas II Congreso Ibérico de Geoquímica, Lisboa*, 329–32.

Medaris, G., Jelínek, E. and Mísar, Z. (1995) Czech eclogites: Terrane settings and implications for Variscan tectonic evolution of the Bohemian Massif. *Eur. J. Mineral.*, **7**, 7–28.

Messiga, B., Tribuzio, R. and Caucia, F. (1992) Amphibole evolution in Varican eclogite-amphibolite from the Savona crystalline massif (Western Ligurian Alps, Italy): Controls on the decompressional *P-T-t* path. *Lithos*, **27**, 215–30.

Mullen, E.D. (1983) $MnO/TiO_2/P_2O_5$: a minor element discriminant for basaltic rocks of oceanic environments and its implications for petrogenesis. *Earth Planet. Sci. Lett.*, **62**, 53–62.

O'Brien, P.J., Röhr, C., Okrusch, M. and Patzak, M. (1992) Eclogite facies relics and a multistage breakdown in metabasites of the KTB pilot hole, NE Bavaria: Implications for the Variscan tectonometamorphic evolution of the NW Bohemian Massif. *Contrib. Mineral. Petrol.*, **112**, 261–78.

Patiño Douce, A.E. and Johnston, A.D. (1991) Phase equilibria and melt productivity in the pelitic system: implications for the origin of peraluminous granitoids and aluminous granulites. *Contrib. Mineral. Petrol.*, **107**, 202–18.

Paulssen, H. and Visser, J. (1993) The crustal structure in Iberia inferred from P-wave coda. *Tectonophysics*, **221**, 111–23.

Pearce, J.A. and Norry, M.J. (1979) Petrogenetic implications of Ti, Zr, Y and Nb variations in

volcanic rocks. *Contrib. Mineral. Petrol.*, **69**, 33–47.

Raheim, A. and Green, D.H. (1975) Experimental determination of the temperature and pressure dependence of the Fe-Mg partition coefficient of coexisting garnet and clinopyroxene. *Contrib. Mineral. Petrol.*, **48**, 179–203.

Ridley, J. (1989) Vertical movement in orogenic belts and the timing of metamorphism relative to deformation. Pp. 103–15 in: *Evolution of Metamorphic Belts* (J.S.J. Daly, R.A. Cliff and B.W.D. Yardley, editors). Spec. Publ., **43**. Geological Society, London.

Ringwood, A.E. (1975) *Composition and Petrology of the Earth's Mantle*. McGraw Hill, New York.

Robinson, P., Spear, F.S., Schumacher, J.C., Laird, J., Klein, C., Evans, B.W. and Doolan, B.L., (1982) Phase relations of metamorphic amphiboles: natural occurrence and theory. Pp. 1–27 in: *Amphiboles and other Hydrous Pyriboles – Mineralogy* (D.R. Veblen and P.H. Ribbe, editors). Reviews in Mineralogy, **9B**. Mineralogical Society of America, Washington DC.

Rollinson, H. (1993) *Using Geochemical Data: Evaluation, Presentation and Interpretation*. Longman, Essex.

Ruppel, C. and Hodges, K.V. (1994) Presssure-temperature-time paths from two-dimensional thermal models: prograde, retrograde, and inverted metamorphism. *Tectonics*, **13**, 17–44.

San José, M.A., Pieren, A.P., García-Hidalgo, J.F., Herranz, P., Peláez, J.R. and Perejón, A. (1990) Central Iberian Zone. Anteordovician Stratigraphy. Pp. 147–59 in: *Pre-Mesozoic Geology of Iberia* (R.D. Dallmeyer and E. Martínez García, editors). Springer Verlag, Berlin.

Saunders, A.D. and Tarney, J. (1984) Geochemical characteristics of basaltic volcanism within back-arc basins. Pp. 59–76 in: *Marginal Basin Geology* (B.P. Kokelar and M.F. Howells, editors). Spec. Publ., **16**. Geological Society, London.

Spear, F.S. (1991) On the interpretation of peak metamorphic temperatures in light of garnet diffusion during cooling. *J. Metam. Geol.*, 9, 379–88.

Spear, F.S. (1993) *Metamorphic Phase Equilibria and Pressure-Temperature-Time Paths*. Monograph of the Mineralogical Society of America, Washington DC.

Sun, S.S. (1980) Lead isotopic study of young volcanic rocks from mid-ocean ridges, ocean islands and islands arcs. *Phil. Trans. R. Soc.*, **A297**, 409–45.

Thompson, A.B., Schulmann, K. and Jezek, J. (1997) Extrusion tectonics and elevation of lower crustal metamorphic rocks in convergent orogens. *Geology*, **25**, 491–4.

Valverde Vaquero, P. Hernáiz, P.P., Escuder, J. and Dunning, G.R. (1995) Comparison of the pre-Cambrian and Paleozoic evolution of the Sierra de Guadarrama (Central Iberian Zone, Spain) and the Gondwana margin, NFLD Appalachians (GMNA). *Terra Abstracts*, **7**, 278.

Viallete, Y., Casquet, C., Fuster, J.M., Ibarrola, E., Navidad, M., Peinado, M. and Villaseca, C. (1987) Geochronological study of orthogneisses from the Sierra de Guadarrama (Spanish Central System). *Neues Jarhb. Mineral. Mh.*, **H10**, 465–79.

Villaseca, C. (1983) *Evolución metamórfica del sector centro-septentrional de la Sierra de Guadarrama*. PhD Thesis, Univ. Complutense de Madrid.

Villaseca, C. (1985) Microdioritas de afinidad toleítica en las bandas de cizalla de Segovia. *Estudios Geológicos*, **41**, 11–5.

Villaseca, C. and Barbero, L. (1994) Estimación de las condiciones del metamorfismo hercínico de alta presión de la Sierra de Guadarrama. *Geogaceta*, **16**, 27–30.

Villaseca, C., Barbero, L. and Rogers, G. (1998) Crustal origin of Hercynian peraluminous granitic batholiths of Central Spain: petrological, geochemical and isotopic (Sr, Nd) constraints. *Lithos*, **43**, 55–79.

Villaseca, C., Barbero, L., Huertas, M.J., Andonaegui, P. and Bellido, F. (1993) *A cross-section through Hercynian granites of the Central Iberian Zone. Excursion Guide*. C. S. I. C., Madrid.

Wildberg, H.D.H., Bischoff, L. and Baumann, A. (1989) U-Pb ages of zircon from meta-igneous and meta-sedimentary rocks of the Sierra de Guadarrama: implications for the Central Iberian crustal evolution. *Contrib. Mineral. Petrol.*, **103**, 253–62.

Willett, S.D., Beaumont, C. and Fullsack, P. (1993) Mechanical models for the tectonics of doubly vergent compressional orogens. *Geology*, **21**, 371–4.

Winkler, H.G.F. (1976) *Petrogenesis of Metamorphic Rocks*. Springer, Berlin.

Wood, B.J. and Banno, S. (1973) Garnet-orthopyroxene and orthopyroxene-clinopyroxene relationships in simple and complex systems. *Contrib. Mineral. Petrol.*, **42**, 109–24.

APPENDIX

Selected equilibria used in TWQEE analysis (Berman, 1991). Numbers refer to those in the intersection diagrams in Fig. 9.

1. Jd + Qz = Ab
2. Py + 2 Grs + 3 Ab = 3 An + 3 Di + 3 Jd
3. 2 Grs + Py + 3 Qz = 3 Di + 3 An (Grt-Cpx-Plg-Qz barometer)
4. Alm + 2 Grs + 3 Qz = 3 Hd + 3 An
5. 3 Ab + Alm + 2Grs = 3 Jd + 3 Hd 3 An
6. Alm + 3 Di = Py + 3 Hd (Grt-Cpx thermometer)
7. 4 Hd + Py + 4 Rt = 3 Qz + 4 Ilm + 3 Di An
8. 2 Rt + Py + 2 Hd + Grs = 2 An + 3 Di + 2 Ilm
9. Alm + 3 Hd + 6 Rt = 6 Qz + 6 Ilm + Grs
10. 6 Rt + Py + 6 Hd = 3 Di + Grs + 6 Ilm

Abbreviations: Ab, albite; An, anortite; Alm, almandine; Di, diopside; Grs, grossular; Hd, hedenbergite; Ilm, ilmenite; Jd, jadeite; Py, pyrope; Qz, beta quartz; Rt, rutile. Other abbreviations follow Kretz (1983).